Supplementary material

Schiff Bases Particles with Aggregation-Induced Enhanced Emission: Random Aggregation Preventing π-π Stacking

Lianke Wang, Zheng Zheng, Zhipeng Yu, Jun Zheng, Min Fang, Jieying Wu, Yupeng Tian and Hongping Zhou,*

College of Chemistry and Chemical Engineering, Anhui University and Key Laboratory of Functional Inorganic Materials Chemistry of Anhui Province, Hefei 230601, P. R. China

**Corresponding author. Fax: +86-551-5107304; Tel: +86-551-5108151*

E-mail address: zhpzhp@263.net.

Table of Contents

Table S1. Relevant Spectroscopic Data of the Schiff Bases in Different Solvents.

Compounds	solvent	λ_2 [a]	ε [b]	λ_{em} [c]	$\Delta\lambda_{ST}$ [d]	λ_1 [a]	ε [b]
L1	benzene	339.0	2.647	379.4	3141.119	302.5	2.762
	CH_2Cl_2	338.0	2.609	380.2	3283.852	302.0	2.656
	THF	338.5	3.0945	378.6	3128.997	302.5	2.901
	ethyl acetate	337.5	2.903	378.4	3202.568	300.5	2.984
	acetonitrile	337.0	2.890	381.8	3481.867	300.5	2.895
	DMF	337.5	2.909	389.4	3949.095	302,0	2.724
L2	benzene	340.0	2.617	377.6	2928.714	303.0	2.248
	CH_2Cl_2	336.0	2.700	378.4	3334.843	301.5	2.819
	THF	338.0	2.754	381.4	3366.606	302.5	2.749
	ethyl acetate	336.0	2.612	378.0	3306.878	301.0	2.673
	acetonitrile	336.5	2.688	379.8	3388.035	300.0	2.712
	DMF	337.0	2.595	387.6	3873.797	303.0	2.517
L3	benzene	342.5	2.233	379.0	2811.856	303.0	2.435
	CH_2Cl_2	341.5	2.532	381.0	3035.858	301.5	2.778
	THF	340.5	2.696	381.8	3176.852	301.0	2.892
	ethyl acetate	338.5	2.536	379.2	3170.789	300.0	2.801
	acetonitrile	336.0	2.586	381.4	3542.712	299.0	2.820
	DMF	339.0	2.866	389.0	3791.584	301.5	3.184

[a] Absorption peak position in nm (1×10^{-5}mol L^{-1}). [b] Maximum molar absorbance in 10^4 mol^{-1} L cm^{-1}. [c] Peak position of SPEF in nm (1.0×10^{-5} mol L^{-1}), excited at the absorption maximum. [d] Stokes shift in nm.

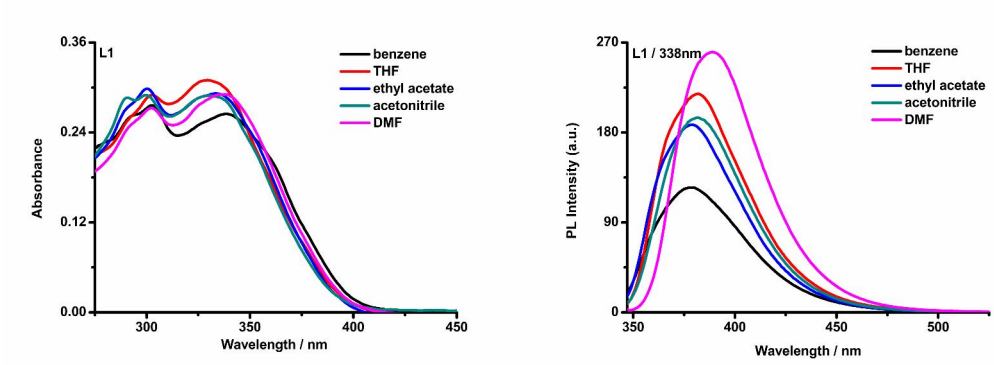

Figure S1. The UV-Vis absorption spectrum (left) and fluorescence emission spectrum (right) of **L1** in different solvents using λ_2 as the excitation wavelength.

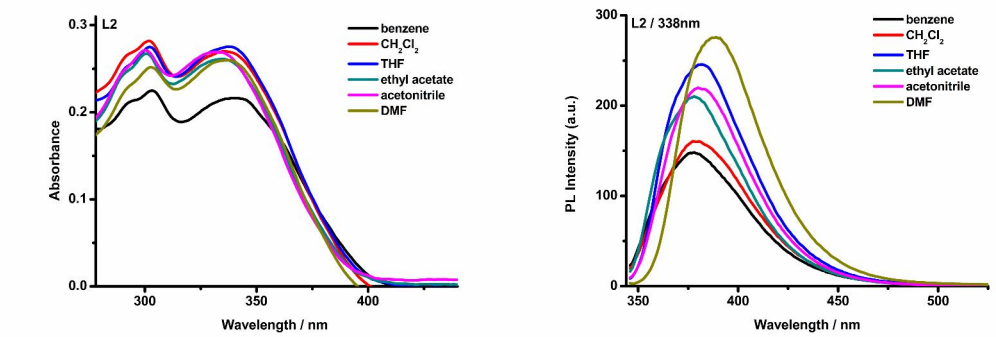

Figure S2. The UV-Vis absorption spectrum (left) and fluorescence emission spectrum (right) of **L2** in different solvents using λ_2 as the excitation wavelength.

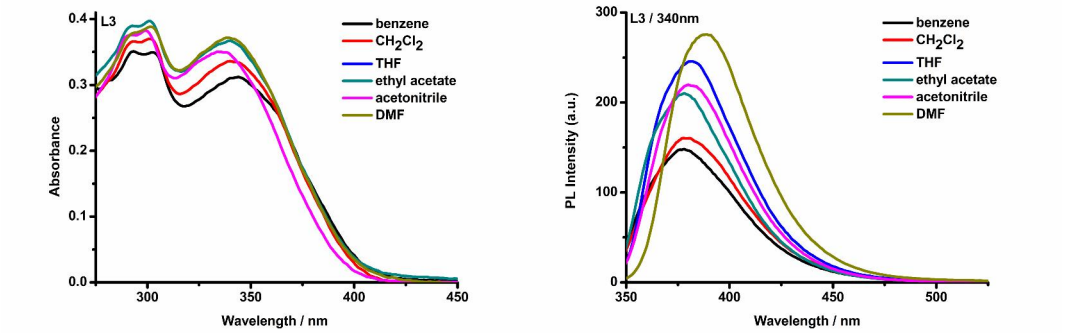

Figure S3. The UV-Vis absorption spectrum (left) and fluorescence emission spectrum (right) of **L3** in different solvents using λ_2 as the excitation wavelength.

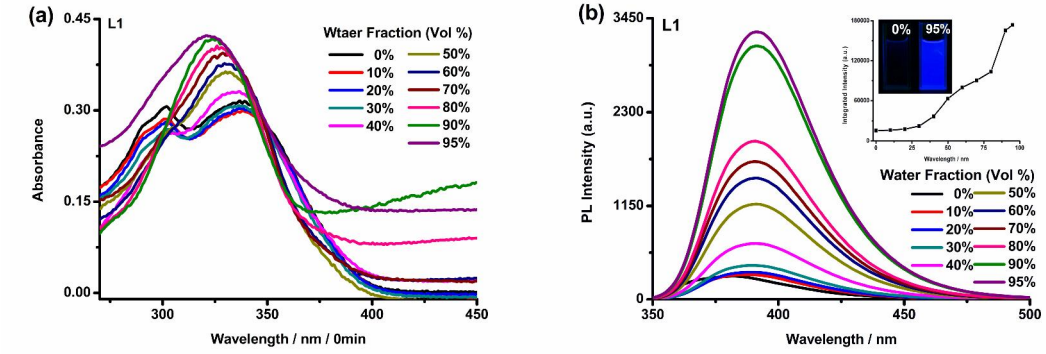

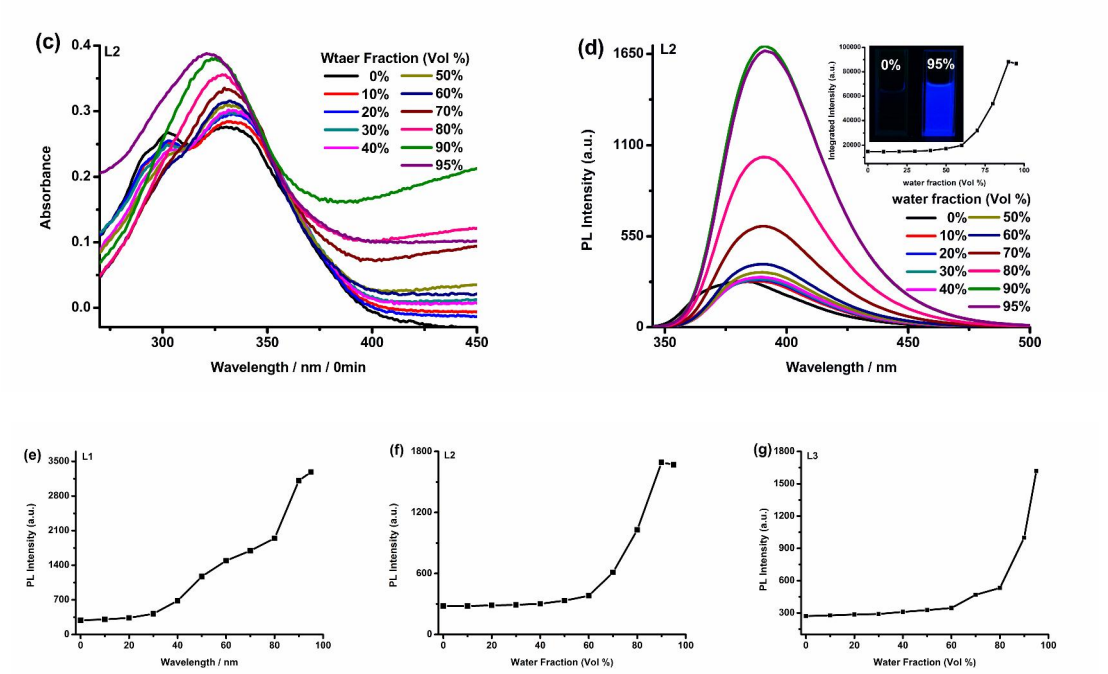

Figure S4. The absorption (a) (c) and emission (b) (d) spectra of **L1** and **L2** in THF/H_2O mixtures with different water fractions (f_w), respectively. The inset depicts the changes of integrated intensity with different water fractions and the photos taken under UV light of **L1** and **L2** in the THF/water mixtures. (e) (f) and (g) depict the changes of PL intensity of **L1**, **L2** and **L3** with different water fractions, respectively.

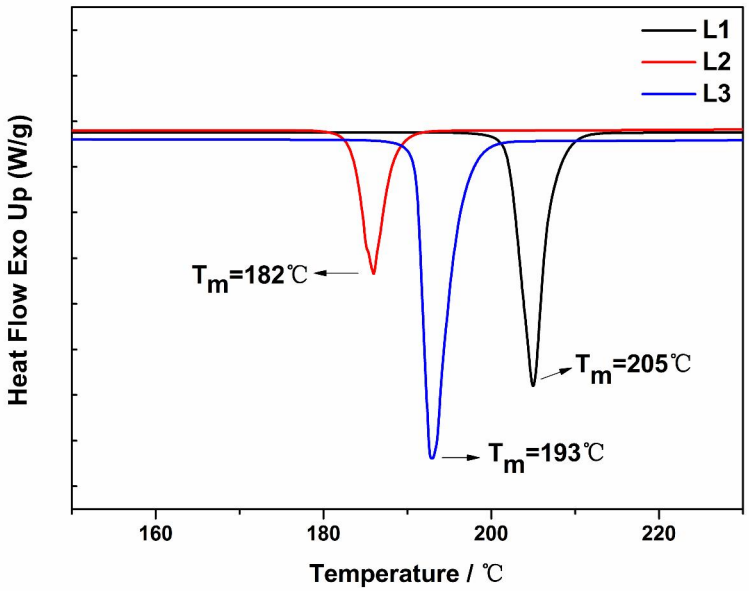

Figure S5. DSC thermograms of **L1**, **L2** and **L3**, heating rate: 20 °C /min, atmosphere: N_2.

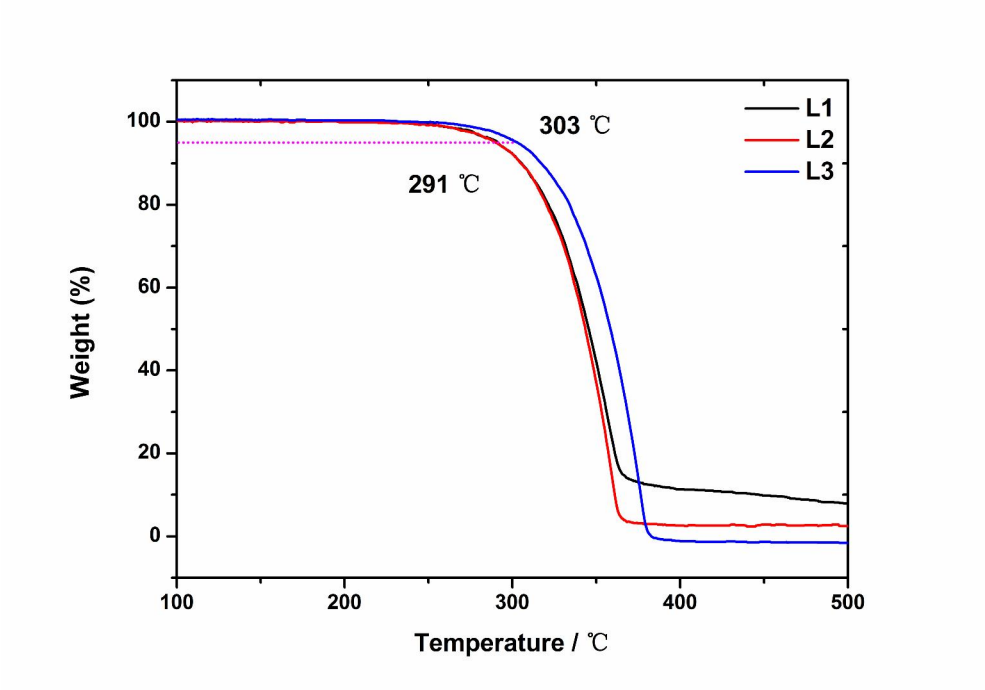

Figure S6. TGA thermograms of **L1**, **L2** and **L3**, recorded after pre-warming at 120 °C for 10 min under nitrogen at a heating rate of 20 °C /min.

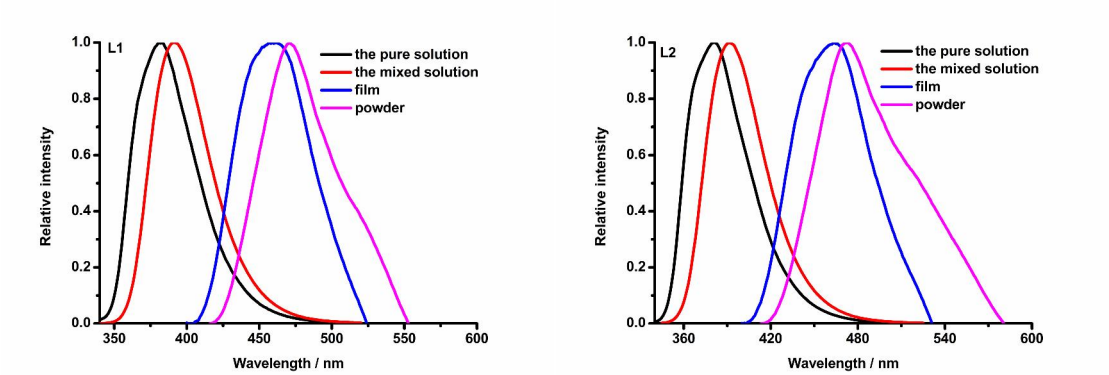

Figure S7. The fluorescent spectroscopy of **L1** and **L2** in the pure solvents, the mixed solution with f_w = 95%, the film, the powder.

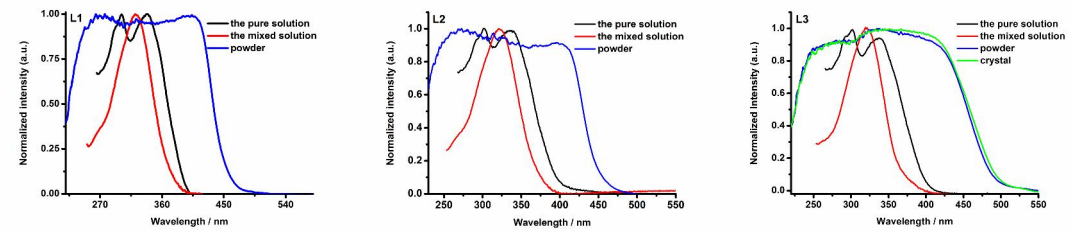

Figure S8. The absorption spectra of **L1**, **L2** and **L3** in the pure solvention, the mixed solution with f_w = 95%, the film, the powder.

Table S2. The average diameter of aggregates with different f_w of **L1-L3**.

L1		**L2**		**L3**	
$d_{fw=50\%}$ (nm)	1696.7	$d_{fw=50\%}$ (nm)	1499	$d_{fw=60\%}$ (nm)	1015.1
$d_{fw=70\%}$(nm)	731.1	$d_{fw=70\%}$(nm)	557	$d_{fw=70\%}$(nm)	569.5
$d_{fw=90\%}$(nm)	353.6	$d_{fw=90\%}$(nm)	301.2	$d_{fw=90\%}$(nm)	310.9
$d_{fw=95\%}$(nm)	288.3	$d_{fw=95\%}$(nm)	255.4	$d_{fw=95\%}$(nm)	249.8

d = average diameter of aggregates with different water fraction.

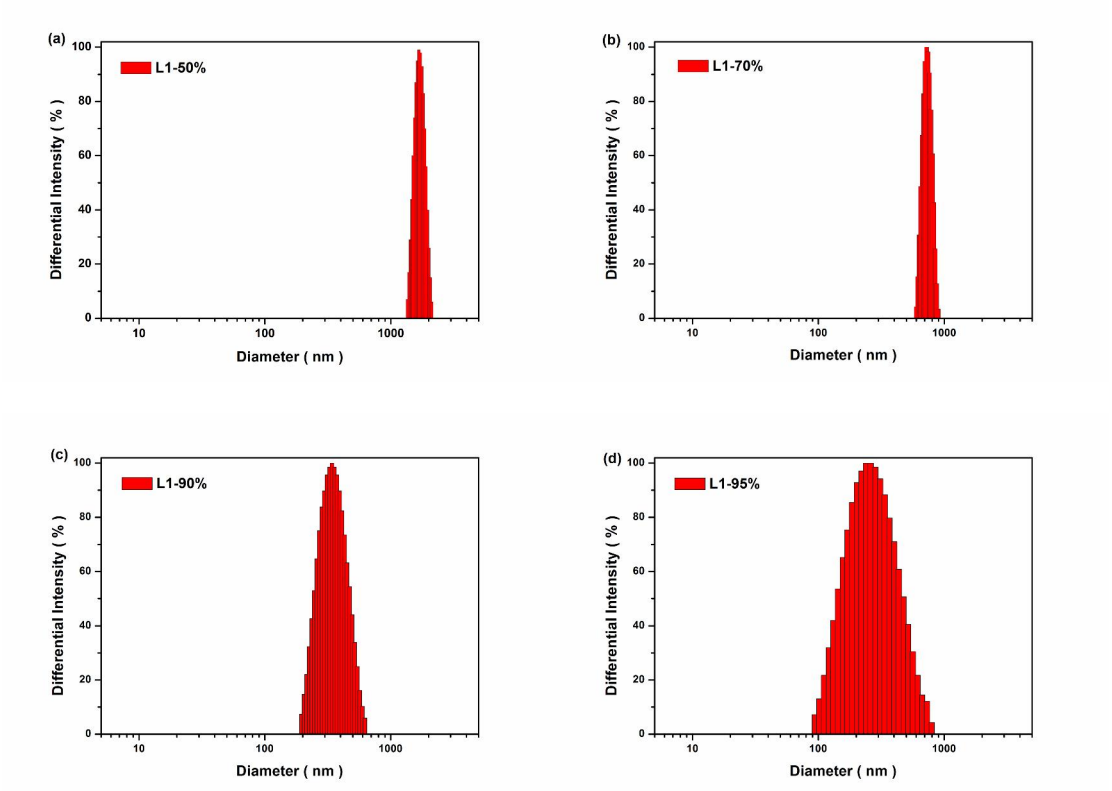

Figure S9. Particle size distributions of **L1** in THF/water mixtures with water fractions of (a) 50%, (b) 70%, (c) 90% and (d) 95%.

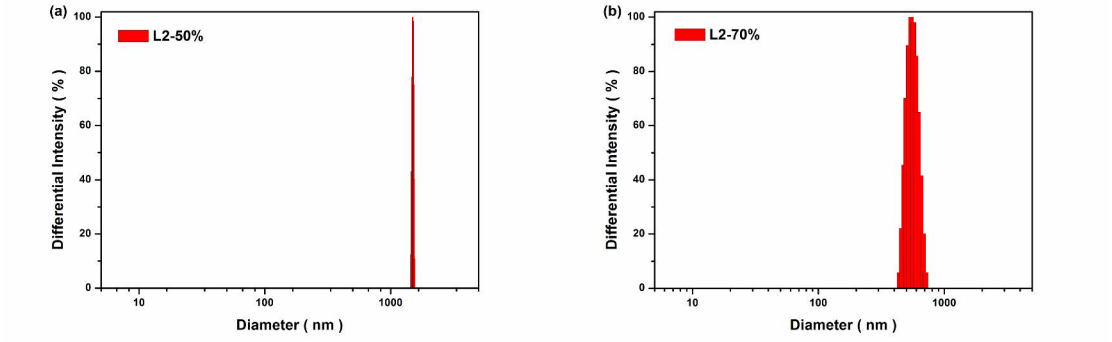

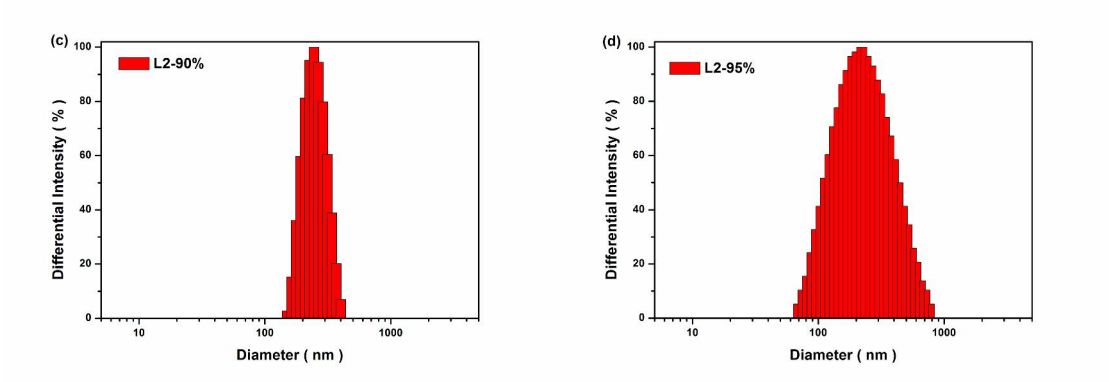

Figure S10. Particle size distributions of **L2** in THF/water mixtures with water fractions of (a) 50%, (b) 70%, (c) 90% and (d) 95%.

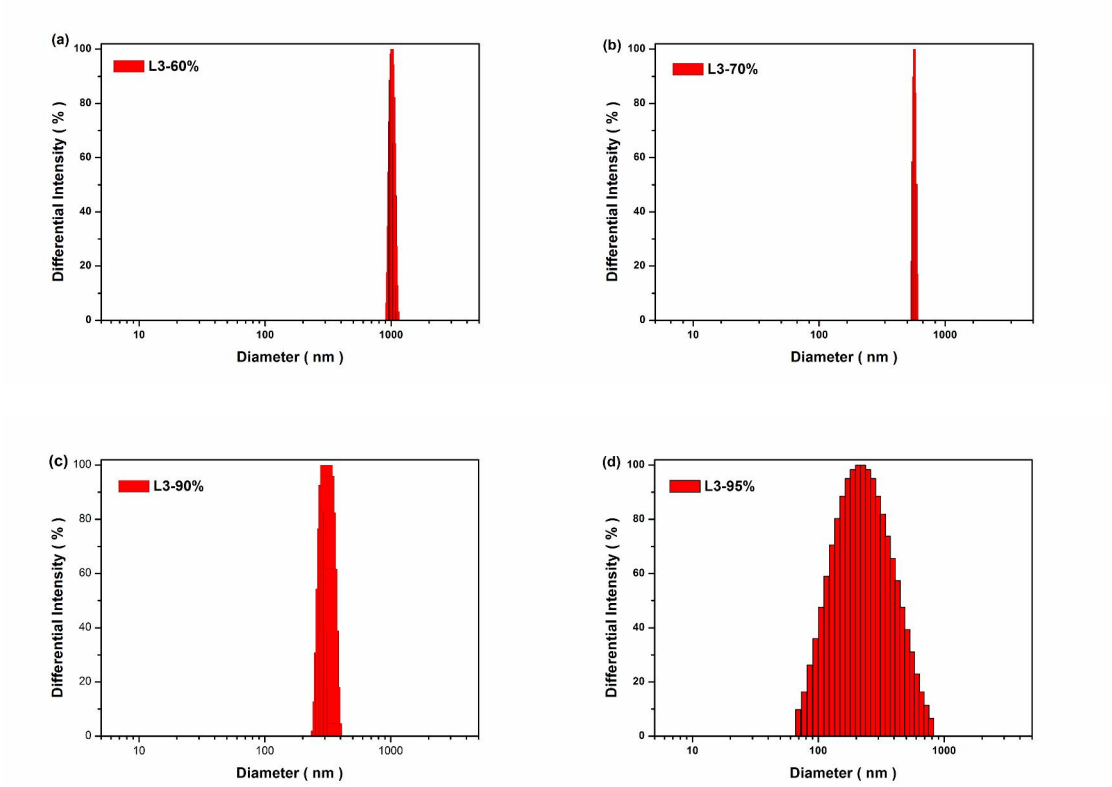

Figure S11. Particle size distributions of **L3** in THF/water mixtures with water fractions of (a) 60%, (b) 70%, (c) 90% and (d) 95%.

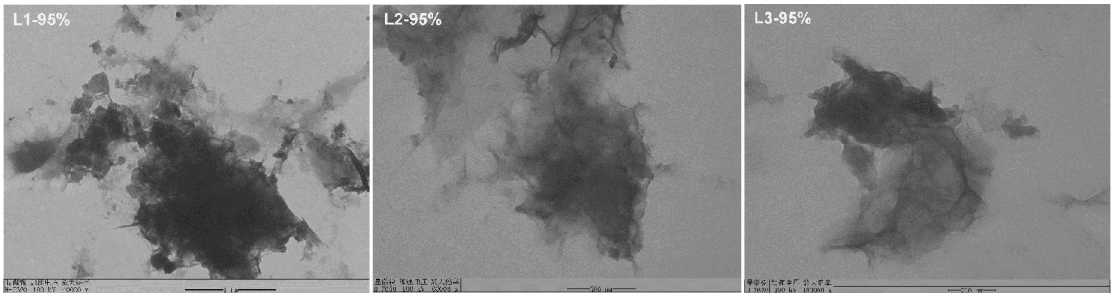

Figure S12. TEM images of amorphous-like aggregates of **L1**, **L2** and **L3** formed in

THF/water mixtures with f_w = 95%.

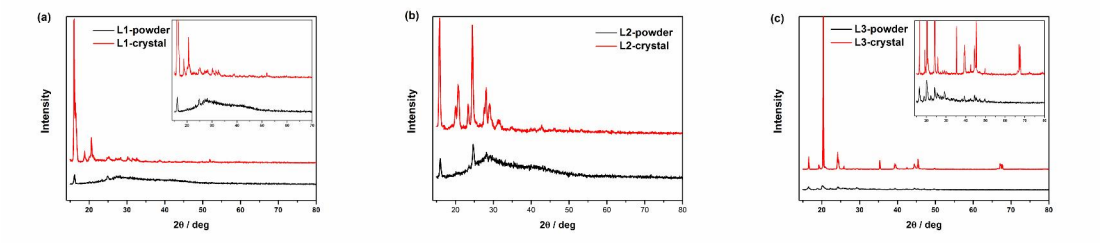

Figure S13. XRD patterns of **L1**, **L2** and **L3** solids.

Table S3. Crystallographic Data for **L3**.

compound	**L3**
empirical formula	$C_{19}H_{13}N_3O$
formula weight	299.32
crystal system	Orthorhombic
space group	*Pbca*
a [Å]	10.969(5)
b [Å]	7.342(5)
c [Å]	36.533(5)
α[°]	90.000(5)
β[°]	90.000(5)
γ[°]	90.000(5)
V [Å^3]	2942(2)
Z	8
T [K]	298(2)
D_{calcd}[g ·cm^{-3}]	1.351
μ [mm^{-1}]	0.086
*θ*range [°]	1.11-24.99
total no. data	19174
no.unique data	2592
no. params refined	208
R_1	0.0378
wR_2	0.1133
GOF	1.115

Figure S14. ^{1}H NMR spectrum of **L1**.

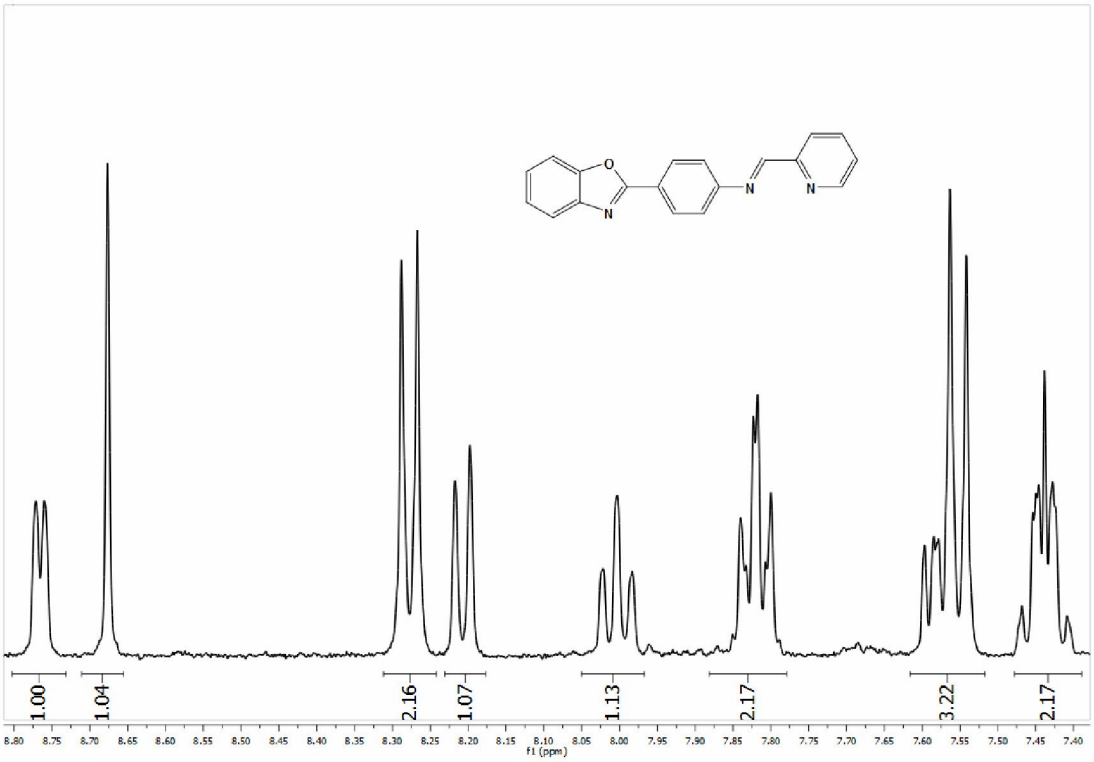

Figure S15. ^{13}C NMR spectrum of **L1**.

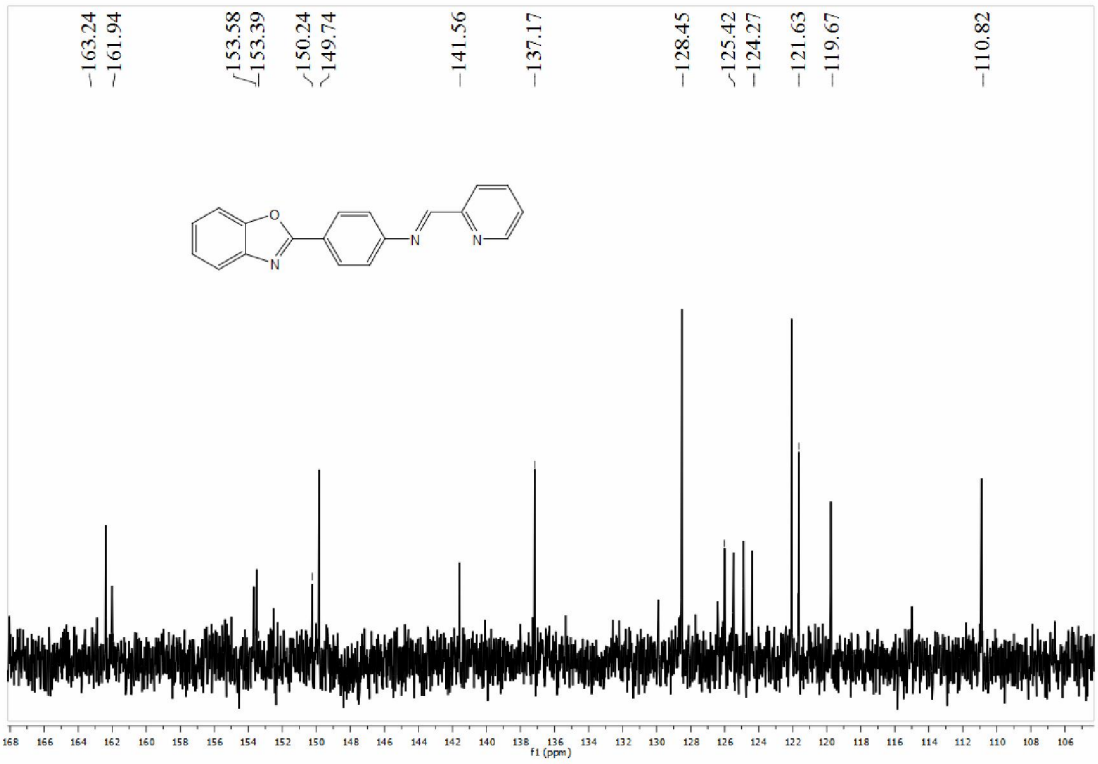

Figure S16. MS spectrum of **L1**.

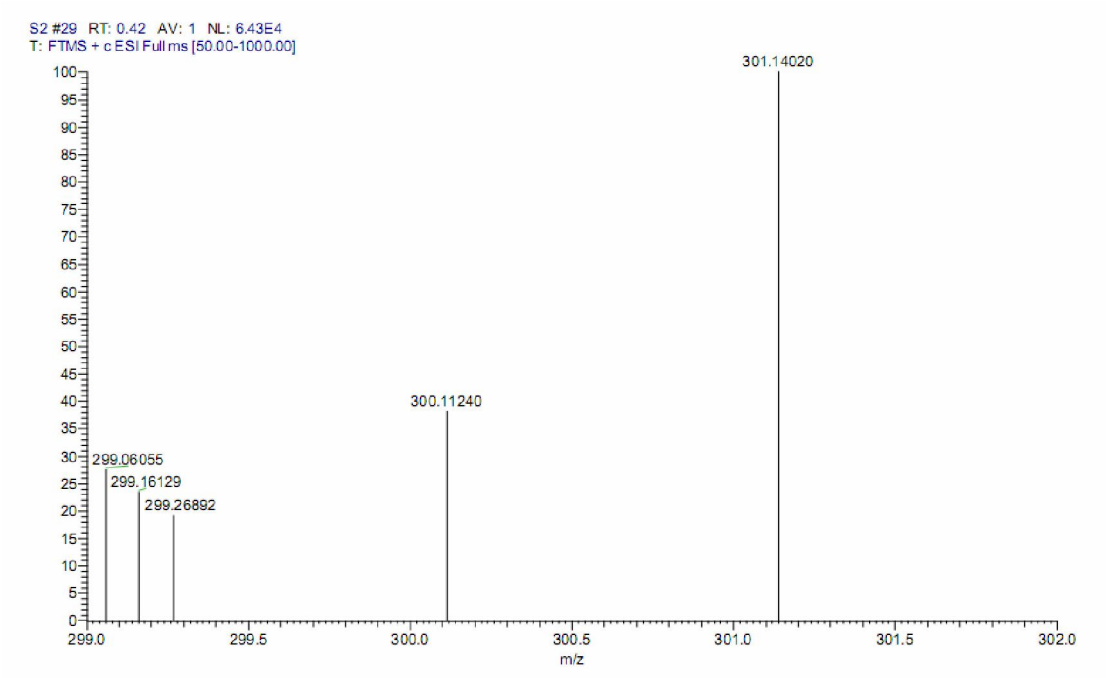

Figure S17. ^{1}H NMR spectrum of **L2**.

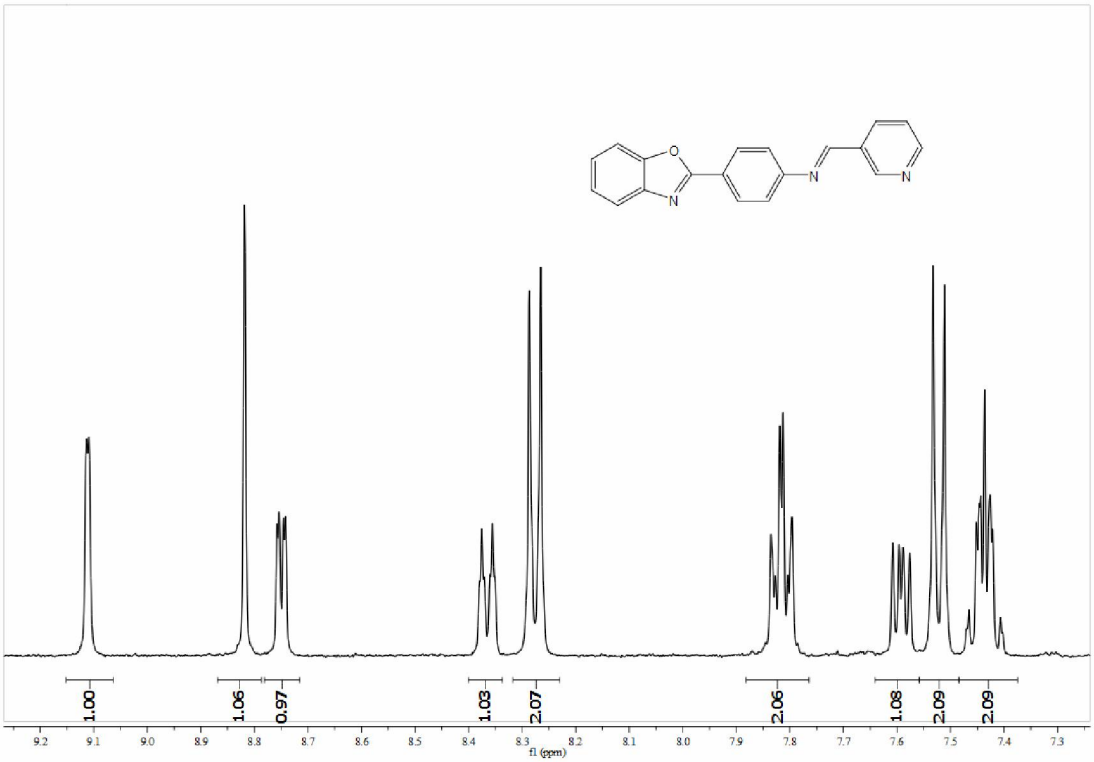

Figure S18. ^{13}C NMR spectrum of **L2**.

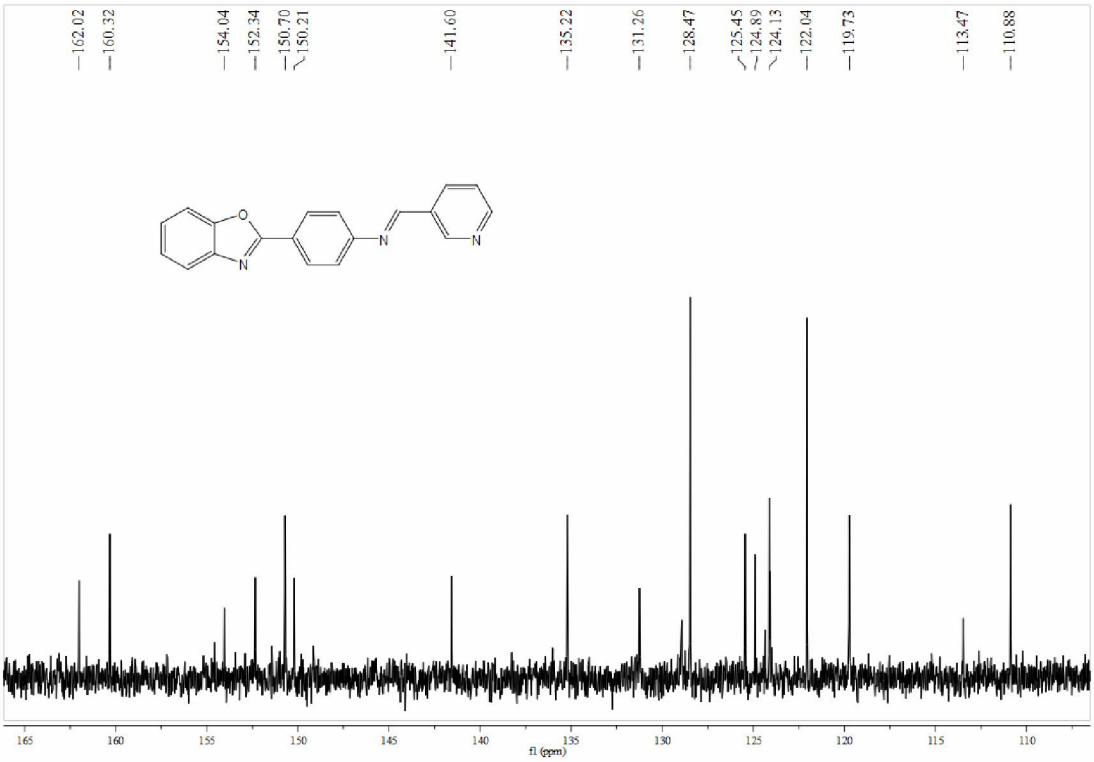

Figure S19. MS spectrum of **L2**.

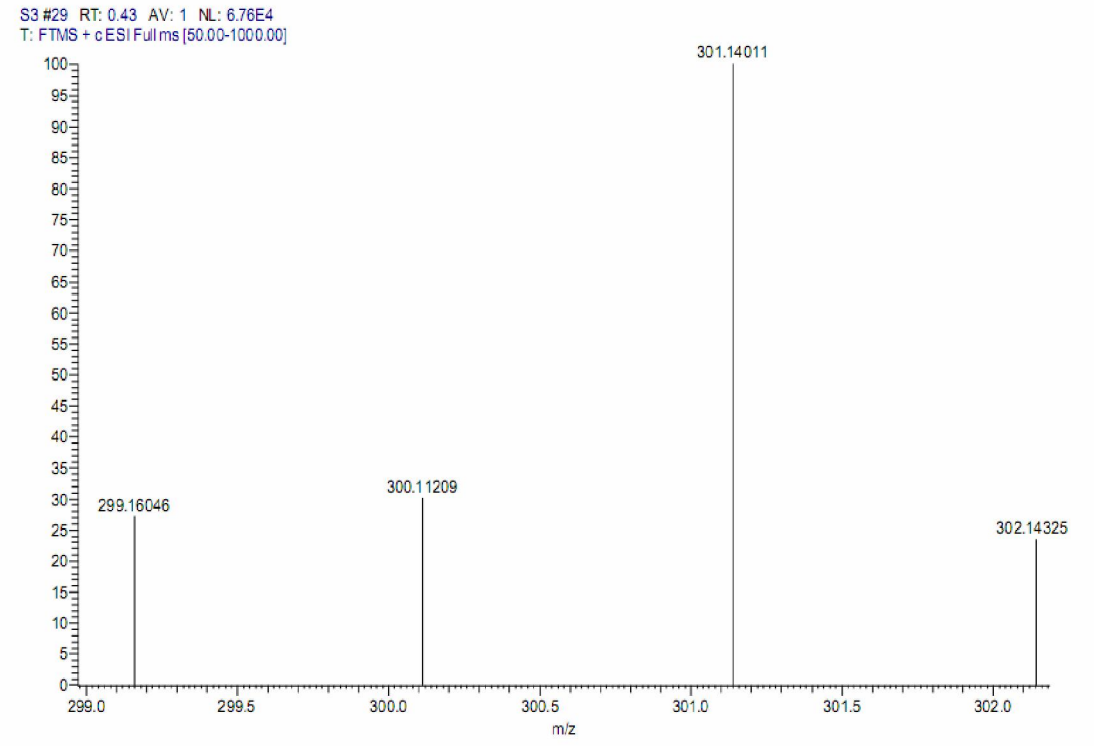

Figure S20. ^{1}H NMR spectrum of **L3**.

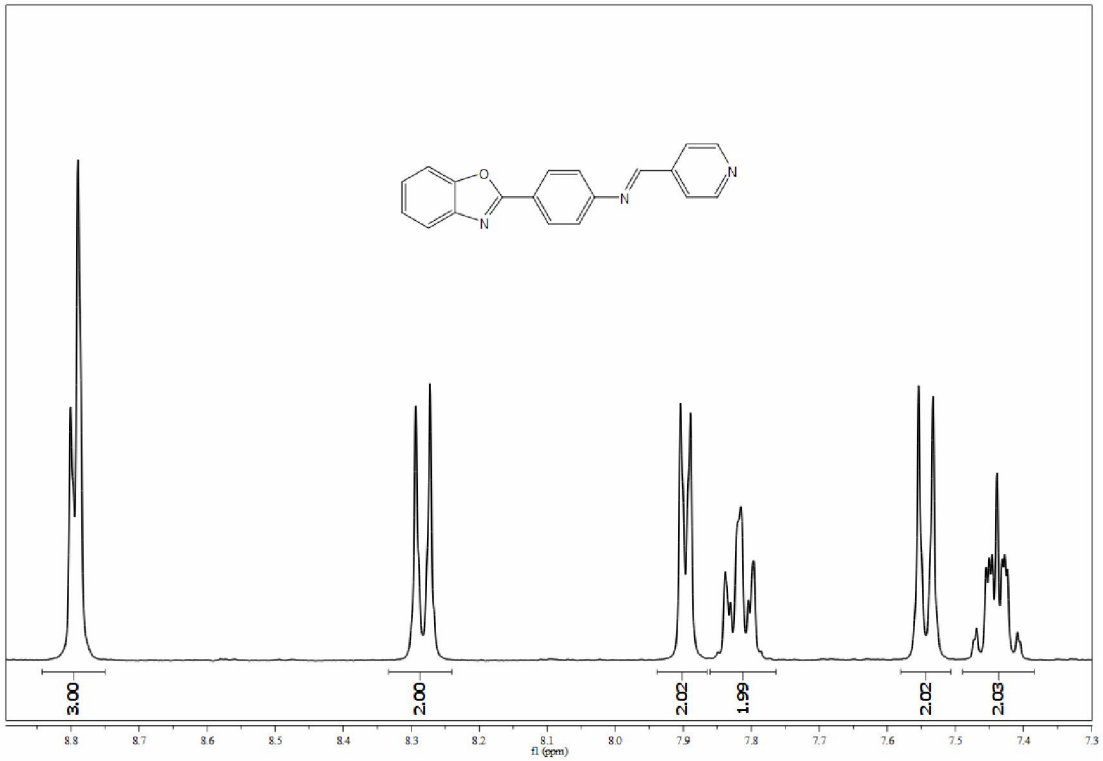

Figure S21. ^{13}C NMR spectrum of **L3**.

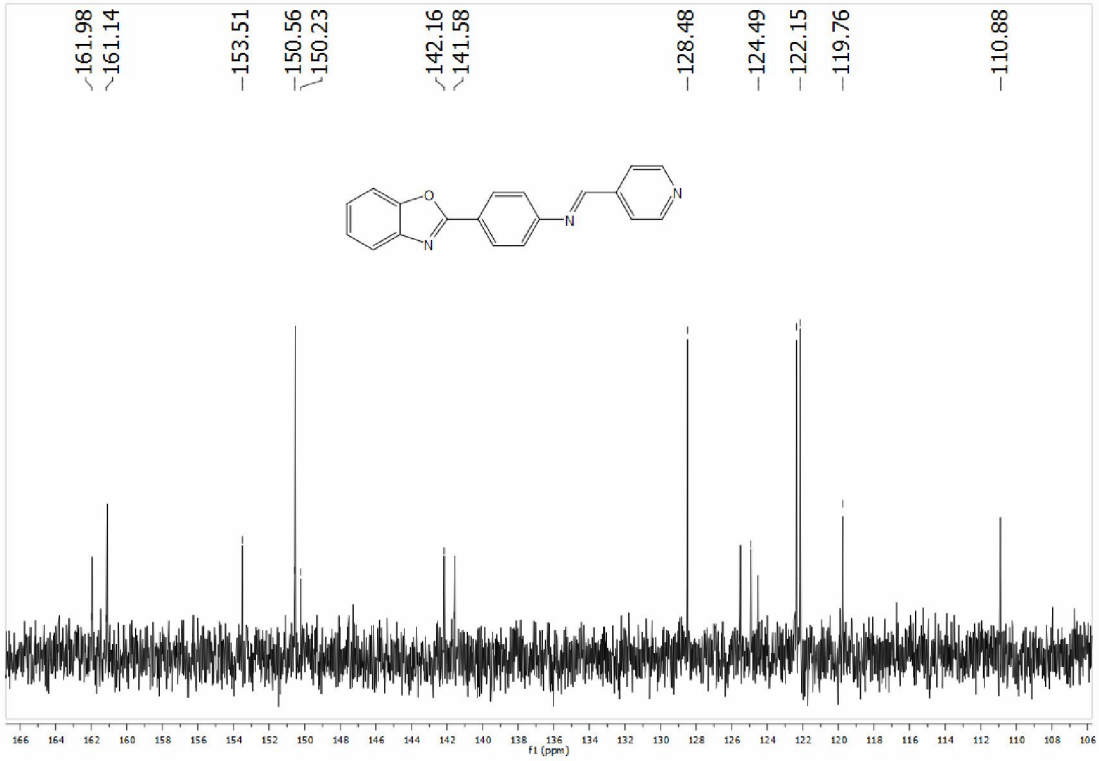

Figure S22. MS spectrum of **L3**.